Observation of the $B_s^0 \to \eta'\eta'$ Decay

R. Aaij et al.[*]

(LHCb Collaboration)

The first observation of the $B_s^0 \to \eta'\eta'$ decay is reported. The study is based on a sample of proton-proton collisions corresponding to 3.0 fb^{-1} of integrated luminosity collected with the LHCb detector. The significance of the signal is 6.4 standard deviations. The branching fraction is measured to be $[3.31 \pm 0.64(\text{stat}) \pm 0.28(\text{syst}) \pm 0.12(\text{norm})] \times 10^{-5}$, where the third uncertainty comes from the $B^\pm \to \eta'K^\pm$ branching fraction that is used as a normalization. In addition, the charge asymmetries of $B^\pm \to \eta'K^\pm$ and $B^\pm \to \phi K^\pm$, which are control channels, are measured to be $(-0.2 \pm 1.3)\%$ and $(+1.7 \pm 1.3)\%$, respectively. All results are consistent with theoretical expectations.

Hadronic decays of beauty hadrons into final states without charm quarks (charmless decays) are suppressed in the standard model of elementary particles. They proceed predominantly through $b \to u$ transitions, mediated by the emission of a virtual $W^\pm$ boson, and $b \to s$ transitions, mediated by the exchange of a virtual $W^\pm$ boson and a virtual quark. The respective "tree" and "penguin" amplitudes are of similar size, allowing for possible large quantum interference effects measurable as charge-parity (CP) violating asymmetries. New particles not described in the standard model may contribute with additional amplitudes, and therefore affect both the decay rates and the CP asymmetries [1]. The $B^\pm \to \eta'K^\pm$ and $B^0 \to \eta'K^0$ decays, first observed by the CLEO Collaboration [2], have some of the largest branching fractions among all charmless hadronic B-meson decays [3]. (Charge conjugation of neutral $B_{(s)}^0$ mesons is implied throughout this Letter. The notations η' and ϕ refer to the $\eta'(958)$ and $\phi(1020)$ mesons, respectively.) Studies of such decays, conducted so far mostly at e^+e^- colliders operating at the $\Upsilon(4S)$ resonance, provide accurate measurements of integrated [4,5] and time-dependent [6,7] CP-violating asymmetries in charmless hadronic $B^\pm$ and B^0 meson decays, and are useful to look for deviations from standard model predictions.

Charmless hadronic B_s^0 decays are poorly known, in particular decays to a pair of unflavoured neutral mesons [8,9], but have been extensively studied in the framework of QCD factorization [10–12], perturbative QCD [13], soft collinear effective theory [14], and flavour SU(3) symmetry [15]. The decay $B_s^0 \to \eta'\eta'$ is expected to have a relatively large branching fraction, similar to that of its SU(3) counterpart $B \to \eta'K$; predictions range between 14×10^{-6}

and 50×10^{-6}, and have large uncertainties [10–15]. The $\eta'\eta'$ final state is a pure CP eigenstate. Decays to this final state of B_s^0 and $\bar{B}_s^0$ mesons flavor tagged at production may therefore be used to investigate time-dependent CP asymmetries in a complementary way to the measurements in $B_s^0 \to \phi\phi$ [16], but without the need for an angular analysis.

In this Letter, we present the first observation of the $B_s^0 \to \eta'\eta'$ decay. Its branching fraction is measured using the known $B^\pm \to \eta'K^\pm$ and $B^\pm \to \phi K^\pm$ decays as calibration channels. The CP asymmetries of the calibration channels are also measured, relatively to the $B^\pm \to J/\psi K^\pm$ channel. All these measurements use proton-proton (pp) collisions corresponding to 3.0 fb^{-1} of integrated luminosity, of which 1.0 (2.0) fb^{-1} was collected in 2011 (2012) at a center-of-mass energy of 7 (8) TeV with the LHCb detector.

The LHCb detector [17] is a single-arm forward spectrometer at the LHC covering the pseudorapidity range $2 < \eta < 5$, designed for the study of particles containing b or c quarks. The detector includes a high-precision tracking system, two ring-imaging Cherenkov detectors used to distinguish different types of charged hadrons, a calorimeter system consisting of scintillating-pad and preshower detectors, an electromagnetic calorimeter and a hadronic calorimeter, and a muon system. The trigger [18] consists of a hardware stage, based on information from the calorimeter and muon systems, followed by a software stage, which applies event reconstruction using information from all the detector subsystems.

Signal $B_s^0 \to \eta'\eta'$, $B^\pm \to \eta'K^\pm$, and $B^\pm \to \phi K^\pm$ candidates are reconstructed through the decays $\eta' \to \pi^+\pi^-\gamma$ and $\phi \to K^+K^-$. Selection requirements are chosen to be as similar as possible for the three channels and are optimized for $B_s^0 \to \eta'\eta'$, maximising the figure of merit $\varepsilon/(a/2 + \sqrt{B})$ [19], where ε is the efficiency for selecting simulated signal events, B is the number of background events in the signal region estimated from the mass sidebands, and $a = 5$

is the target significance of the possible signal. The requirements on the ϕ meson and on the charged kaon associated with the η' or ϕ resonance in the candidate $B^{\pm}$ decays, which is referred to as the bachelor kaon, are chosen to minimise the relative statistical uncertainty on the $B^{\pm} \to \phi K^{\pm}$ signal yield.

Charged particles are required to be inconsistent with originating from a primary pp interaction vertex (PV) and to have a transverse momentum (p_T) with respect to the beam line in excess of 0.25 GeV/c, while bachelor kaons must have $p_T > 1.2$ GeV/c. Particle identification algorithms are applied to distinguish kaons from pions, and photons from electrons [20]. Photons are required to have $p_T > 0.5$ GeV/c. The intermediate η' (ϕ) resonances must have $p_T > 1.5(0.5)$ GeV/c and momentum $p > 4$ GeV/c. The $\pi^+\pi^-$ invariant mass in candidate η' decays must exceed 0.56 GeV/c^2. B-meson candidates must have $p_T > 4$ GeV/c. Topological variables are used to isolate the signal, such as the angle between the reconstructed B momentum and the vector pointing from the PV to the B decay vertex (required to be smaller than 10 mrad), and the distance of closest approach to the PV of the B trajectory (required to be less than 0.04 mm). Reconstructed invariant masses of the B_s^0, $B^{\pm}$, η', and ϕ candidates are required to be in the ranges $5000 < m_{B_s^0} < 5600$ MeV/c^2, $5000 < m_{B^{\pm}} < 5500$ MeV/c^2, $880 < m_{\eta'} < 1040$ MeV/c^2 and $1000 < m_{\phi} < 1050$ MeV/c^2, respectively. Only candidates with a well reconstructed B decay vertex are retained; in the events with multiple candidates ($\lesssim 5\%$), the candidate with the smallest vertex χ^2 is kept.

The $B_s^0 \to \eta'\eta'$ signal yield is determined from a multidimensional unbinned extended maximum likelihood fit to the sample of $B_s^0 \to \eta'\eta'$ and $B^{\pm} \to \eta'K^{\pm}$ candidates, using the combined $\sqrt{s} = 7$ and 8 TeV data sets. The likelihood is written as $\mathcal{L} = \exp(-\sum_j N_j) \prod_i^N (\sum_j N_j P_j^i)$, where N_j is the yield of fit component j (signal or backgrounds), P_j^i is the probability of event i for component j, and N is the total number of events. The probabilities P_j^i are expressed as products of probability density functions (PDF) for the invariant masses used as observables in the fit: the $\eta'\eta'$ invariant mass ($m_{\eta'\eta'}$), the two randomly ordered $\pi^+\pi^-\gamma$ invariant masses ($m_{(\pi\pi\gamma)_1}$ and $m_{(\pi\pi\gamma)_2}$) of the $B_s^0 \to \eta'\eta'$ candidates, and the $\eta'K^{\pm}$ and $\pi^+\pi^-\gamma$ invariant masses ($m_{\eta'K}$ and $m_{\pi\pi\gamma}$) of the $B^{\pm} \to \eta'K^{\pm}$ candidates. In the reconstruction of the $\pi^+\pi^-\gamma$ candidates, the known η' mass [3] is applied as a constraint to calculate the $m_{\eta'\eta'}$ and $m_{\eta'K}$ variables.

The $B^{\pm} \to \eta'K^{\pm}$ sample is described with three components: the signal, and two combinatorial background components with and without an η' resonance in the decay chain. The $B_s^0 \to \eta'\eta'$ sample is modeled with seven components, three of which are significant: the signal, the combinatorial background and partially reconstructed b-hadron decays without η' resonances in the final state.

The remaining backgrounds, for which the event yields are found to be consistent with zero, consist of two combinatorial and two partially reconstructed components, each involving only one resonant $\pi^+\pi^-\gamma$ candidate.

All the PDFs that peak at the B or η' mass are modeled by Crystal Ball (CB) functions [21] modified such that both the high- and low-mass tails follow power laws and account for non Gaussian reconstruction effects. The parameters used for the description of $m_{\eta'K}$ for the $B^{\pm}$ signal are free in the fit, while all the parameters of $m_{\eta'\eta'}$ for the B_s^0 signal PDF are determined from simulation, except the CB width. The ratio of the CB widths in $m_{\eta'K}$ and $m_{\eta'\eta'}$ is fixed to that measured in simulation. The partially reconstructed background is described with an ARGUS function [22] convolved with a Gaussian resolution function of the same width as the corresponding signal PDF, while the combinatorial background is modeled with a linear function. A common CB function is used for modeling all the η' resonances, with mean and width free in the fit, while tail parameters are determined from simulation. The mass distribution of η' candidates from random combinations is modeled with an empirical quadratic function.

We observe $36.4 \pm 7.8(\text{stat}) \pm 1.6(\text{syst})$ $B_s^0 \to \eta'\eta'$ decays corresponding to a significance of 6.4 standard deviations, including both statistical and systematic uncertainties, discussed later. The significance is computed using Wilks' theorem [23], and is scaled by the ratio of the statistical over the total uncertainties. The measured $B^{\pm} \to \eta'K^{\pm}$ yield is 8672 ± 114, where the uncertainty is statistical only. Mass distributions are shown in Figs. 1 and 2, with the fit results overlaid.

To measure the ratio of the branching fractions $\mathcal{B}(B_s^0 \to \eta'\eta')/\mathcal{B}(B^{\pm} \to \eta'K^{\pm})$, the fit is repeated taking into account the different reconstruction efficiencies in the 7 and 8 TeV data sets. The four background components with yields consistent with zero are neglected in this case. The common parameters between the 7 and 8 TeV data sets are the shape parameters and the ratio of branching fractions. The ratio of branching fractions is related to the ratio of yields according to

$$
\begin{aligned}
\frac{\mathcal{B}(B_s^0 \to \eta'\eta')}{\mathcal{B}(B^{\pm} \to \eta'K^{\pm})} &= \frac{f_d}{f_s} \times \frac{1}{\mathcal{B}(\eta' \to \pi^+\pi^-\gamma)} \\
&\times \frac{N_l(B_s^0 \to \eta'\eta')}{N_l(B^{\pm} \to \eta'K^{\pm})} \times \frac{\varepsilon_l(B^{\pm} \to \eta'K^{\pm})}{\varepsilon_l(B_s^0 \to \eta'\eta')},
\end{aligned}
\tag{1}
$$

where the subscript l indicates the 7 TeV or 8 TeV data set, the ratio of probabilities for a b quark to produce a B_s^0 or $B^{\pm}$ meson is $f_s/f_d = 0.259 \pm 0.015$ [24], and the branching fraction of the η' decay is $\mathcal{B}(\eta' \to \pi^+\pi^-\gamma) = 0.291 \pm 0.005$ [3]. The ratio of efficiencies for reconstructing the normalization and signal decay channels $\varepsilon_l(B^{\pm} \to \eta'K^{\pm})/\varepsilon_l(B_s^0 \to \eta'\eta')$ is determined from control samples (particle
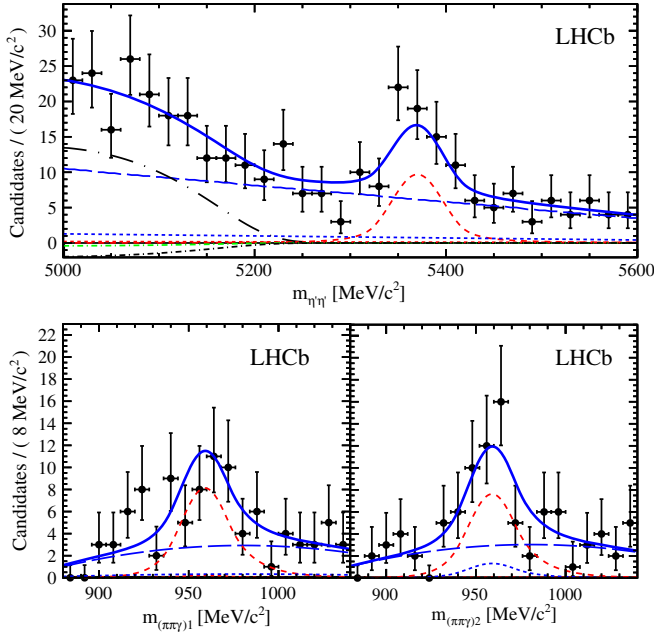
FIG. 1 (color online).   Distributions of the (top) $\eta'\eta'$, (bottom) $(\pi\pi\gamma)_1$ and $(\pi\pi\gamma)_2$ invariant masses for the $B_s^0 \to \eta'\eta'$ candidates with fit results overlaid. The $(\pi\pi\gamma)_1$ and $(\pi\pi\gamma)_2$ mass distributions are shown for the candidates with an $\eta'\eta'$ invariant mass within three standard deviations of the B_s^0 mass. The components are the following: (dashed red curves) $B_s^0 \to \eta'\eta'$ signal, (long-dashed blue curves) combinatorial background without an η' resonance in the final state, (dot-long-dashed black curves) partially reconstructed background without an η' resonance, (short-dashed red, short-dashed blue curves) combinatorial background with one η' resonance, and (dot-dashed green, dot-dashed black curves) partially reconstructed background with one η' resonance. The total fit function is shown as the solid blue curves.

FIG. 2 (color online).   Distributions of the (top) $\eta'K^\pm$ and (bottom) $\pi^+\pi^-\gamma$ invariant masses for the $B^\pm \to \eta'K^\pm$ candidates with fit results overlaid. The components are the following: (dashed red curves) $B^\pm \to \eta'K^\pm$ signal, (long-dashed blue curves) combinatorial background without an η' resonance in the final state, and (dotted blue curves) combinatorial background with an η' resonance. The total fit function is shown as the solid blue curves.

identification, photon reconstruction and hardware trigger on the signal) and simulation to be 8.46 ± 0.35 for the 7 TeV and 7.85 ± 0.26 for the 8 TeV data sets, including all experimental systematic uncertainties. The largest uncertainty in the determination of the efficiency ratio comes from the photon reconstruction efficiency. This efficiency is measured using $B^\pm \to J/\psi K^{*\pm}$ decays followed by $J/\psi \to \mu^+\mu^-$ and $K^{*\pm} \to K^\pm \pi^0 \to K^\pm \gamma\gamma$ [25], and a crosscheck is provided by the measurement of the ratio of branching fractions of the $B^\pm \to \eta'K^\pm$ and $B^\pm \to \phi K^\pm$ control channels. The result of Eq. (1) is then

$$\frac{\mathcal{B}(B_s^0 \to \eta'\eta')}{\mathcal{B}(B^\pm \to \eta'K^\pm)} = 0.47 \pm 0.09\text{(stat)} \pm 0.04\text{(syst)}.$$

Contributions to the systematic uncertainties are summed in quadrature leading to a total systematic uncertainty on the $B_s^0 \to \eta'\eta'$ signal yield (ratio of branching fractions) of 1.6 (0.041). The uncertainties on f_s/f_d, $\mathcal{B}(\eta' \to \pi^+\pi^-\gamma)$, $\varepsilon_l(B^\pm \to \eta'K^\pm)/\varepsilon_l(B_s^0 \to \eta'\eta')$, and on the values of fit model parameters fixed from simulation, lead to a systematic uncertainty of 0.7 (0.038), while a variation
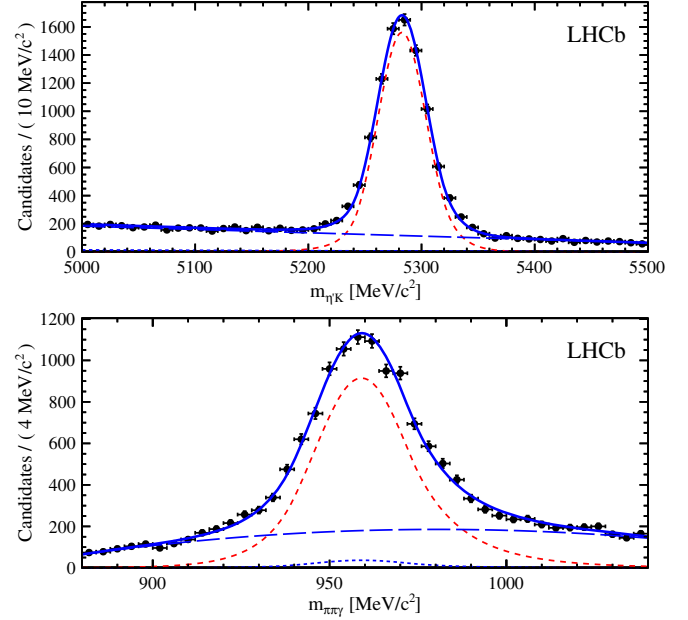
of the PDF models leads to an uncertainty of 1.4 (0.007). The fit bias, evaluated in simulation, is consistent with zero, and its statistical uncertainty of 0.4 (0.005) is applied as a systematic uncertainty. Finally, an uncertainty of 0.014 is assigned to account for the neglected background components in the branching-fraction fit.

Using the known value $\mathcal{B}(B^\pm \to \eta'K^\pm) = (7.06 \pm 0.25) \times 10^{-5}$ [3], the branching fraction is measured to be $\mathcal{B}(B_s^0 \to \eta'\eta') = [3.31 \pm 0.64\text{(stat)} \pm 0.28\text{(syst)} \pm 0.12\text{(norm)}] \times 10^{-5}$, where the third uncertainty comes from the $B^\pm \to \eta'K^\pm$ branching fraction.

The $B^\pm \to \eta'K^\pm$ and $B^\pm \to \phi K^\pm$ charge asymmetries, $\mathcal{A}^{CP} \equiv (\Gamma^- - \Gamma^+)/(\Gamma^- + \Gamma^+)$, where $\Gamma^\pm$ is the partial width of the $B^\pm$ meson, are determined using the strategy adopted in Ref. [26]. For these measurements, we consider either events triggered on signal candidates (TOS events) or events triggered at the hardware stage independently of the signal candidate (non-TOS events). The raw asymmetries $\mathcal{A}^{CP}_{\text{raw}}$ are obtained from a fit to the positively and negatively charged candidates, and each subsample is further split into TOS and non-TOS events, to account for trigger-dependent detection asymmetries [26]. For each channel a two-dimensional fit of the mass distributions of the B candidate and its neutral daughter is performed, and the four samples are fitted simultaneously.

The model in the $B^\pm \to \eta'K^\pm$ fit is the same as that used in the simultaneous $B_s^0 \to \eta'\eta'$ and $B^\pm \to \eta'K^\pm$ fit; the

$B^\pm \to \phi K^\pm$ model mirrors that of Ref. [26], except for the $m_{\phi K}$ signal PDF, which is described by the sum of a CB function and a Gaussian function. The shape parameters used to describe the peaking and partially reconstructed component PDFs are shared, while independent parameters are used for the combinatorial component PDFs in the trigger subsamples. In both fits, each component has four yields parametrized as $N_k^\pm = N_k(1 \mp \mathcal{A}_{\text{raw},k}^{CP})/2$, where N_k and $\mathcal{A}_{\text{raw},k}^{CP}$ are the yield and the raw asymmetry in each trigger category k, respectively.

The observed $B^\pm \to \eta' K^\pm$ ($B^\pm \to \phi K^\pm$) raw asymmetries and their statistical uncertainties are -0.019 ± 0.014 ($+0.003 \pm 0.014$) and -0.027 ± 0.020 (-0.011 ± 0.018) for the TOS and non-TOS categories, respectively, the fraction of event in the TOS category being 63.8% (60.1%). The fitted mass spectra for the $B^\pm \to \phi K^\pm$ candidates are shown in Fig. 3.

In order to determine the CP asymmetry, the raw asymmetry is corrected for the $B^\pm$ production asymmetry in pp collisions, $\mathcal{A}_P$, and for the bachelor $K^\pm$ detection asymmetry due to interactions with the detector matter, $\mathcal{A}_{D,k}$. Under the assumption that these asymmetries are small, $\mathcal{A}_{\text{raw},k}^{CP}$ is related to the CP asymmetry $\mathcal{A}^{CP}$ as $\mathcal{A}_{\text{raw},k}^{CP} = \mathcal{A}^{CP} + \mathcal{A}_{D,k} + \mathcal{A}_P$. Because the CP-violating asymmetry in $B^\pm \to J/\psi K^\pm$ is known precisely [3], the
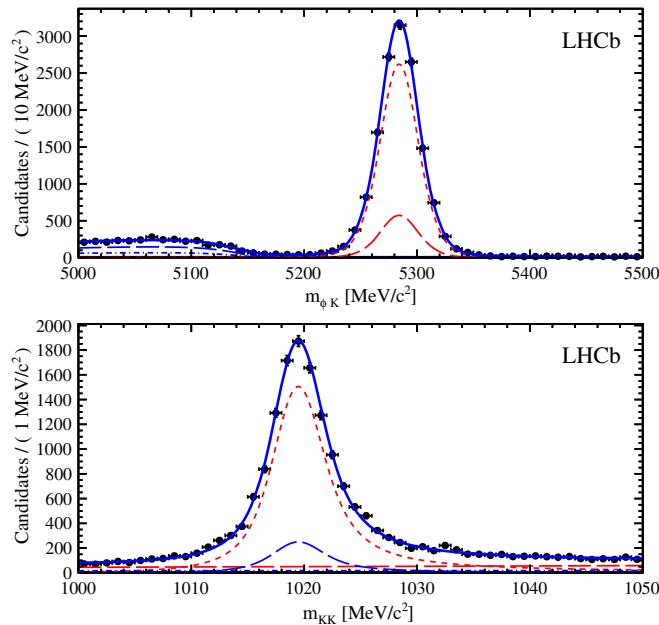

FIG. 3 (color online). Distributions of the (top) $\phi K^\pm$ and (bottom) $K^+ K^-$ invariant masses for the $B^\pm \to \phi K^\pm$ candidates with fit results overlaid The components are the following: (dashed red curves) $B^\pm \to \phi K^\pm$ signal, (long-dashed red curves) nonresonant $B^\pm \to K^+ K^- K^\pm$ background, partially reconstructed b-hadron background (long-dashed blue curves) with or (dot-dashed blue curves) without a ϕ resonance in the decay chain. The combinatorial background with or without a ϕ resonance is too small to be visible. The total fit function is shown as the solid blue curves.

raw asymmetry in this decay is used to determine the sum of the detection and production asymmetries. The raw asymmetry of the $B^\pm \to J/\psi K^\pm$ decay is measured in a simultaneous fit to the $m_{J/\psi K^\pm}$ distributions of the positively and negatively charged candidates selected with similar criteria as for the signal modes. Independent fits are performed for events belonging to each trigger category. The fit model consists of a peaking signal component, described with the sum of a CB function and a Gaussian function, and a linear combinatorial background component.

The raw $B^\pm \to J/\psi K^\pm$ asymmetries, $-0.020 \pm 0.004(\text{stat})$ and $-0.011 \pm 0.003(\text{stat})$ for the TOS and non-TOS categories, respectively, are subtracted from the $B^\pm \to \eta' K^\pm$ or $B^\pm \to \phi K^\pm$ raw asymmetries for each trigger category. The weighted average of these asymmetry differences, $\Delta \mathcal{A}^{CP} = \mathcal{A}^{CP} - \mathcal{A}^{CP}(B^\pm \to J/\psi K^\pm)$, is computed with weights given by the fractions of signal events in each of the two categories. The resulting asymmetry differences are $\Delta \mathcal{A}^{CP}(B^\pm \to \eta' K^\pm) = -0.005 \pm 0.012(\text{stat})$ and $\Delta \mathcal{A}^{CP}(B^\pm \to \phi K^\pm) = +0.014 \pm 0.011(\text{stat})$.

Three significant sources of systematic uncertainties are identified. The first accounts for the effect of the mass shape modeling, leading to an uncertainty on $\Delta \mathcal{A}^{CP}$ of 0.021×10^{-2} (0.20×10^{-2}) for the $B^\pm \to \eta' K^\pm$ ($B^\pm \to \phi K^\pm$) channel. To account for the different kinematic properties between the signal channels and the $B^\pm \to J/\psi K^\pm$ channel, $\Delta \mathcal{A}^{CP}$ is measured in three independent subsamples selected according to the transverse momentum of the bachelor kaon, and their average, weighted by the number of events in each subsample, is computed. The difference from the result obtained in the default fit is 0.018×10^{-2} (0.08×10^{-2}), which is assigned as a systematic uncertainty. Finally, the CP measurements are repeated applying a geometrical requirement [26] to suppress possible detector edge effects. The associated systematic uncertainty is 0.13×10^{-2} (0.05×10^{-2}).

Using the known $B^\pm \to J/\psi K^\pm$ CP asymmetry, $\mathcal{A}^{CP}(B^\pm \to J/\psi K^\pm) = (+0.3 \pm 0.6) \times 10^{-2}$ [3], the asymmetries are measured to be $\mathcal{A}^{CP}(B^\pm \to \eta' K^\pm) = [-0.2 \pm 1.2(\text{stat}) \pm 0.1(\text{syst}) \pm 0.6(\text{norm})] \times 10^{-2}$ and $\mathcal{A}^{CP}(B^\pm \to \phi K^\pm) = [+1.7 \pm 1.1(\text{stat}) \pm 0.2(\text{syst}) \pm 0.6(\text{norm})] \times 10^{-2}$, where the third uncertainty comes from the $B^\pm \to J/\psi K^\pm$ CP asymmetry. These results are compatible with the hypothesis of CP symmetry and with the standard model predictions [12,27].

In conclusion, this Letter presents the first observation of the decay $B_s^0 \to \eta' \eta'$, with a significance of 6.4 standard deviations, and the most precise measurements of CP-violating charge asymmetries in $B^\pm \to \eta' K^\pm$ and $B^\pm \to \phi K^\pm$ decays. The latter result supersedes the previous LHCb measurement [26]. The measured $B_s^0 \to \eta' \eta'$ branching fraction, $\mathcal{B}(B_s^0 \to \eta' \eta') = [3.31 \pm 0.64(\text{stat}) \pm 0.28(\text{syst}) \pm 0.12(\text{norm})] \times 10^{-5}$, agrees with the theoretical predictions. This newly observed B_s^0 decay channel to a charmless CP eigenstate opens possibilities for further

constraining the standard model with time-dependent *CP* asymmetry measurements.

[1] D. Zhang, Z. Xiao, and C. S. Li, Branching ratios and *CP*-violating asymmetries of $B_s \rightarrow h_1 h_2$ decays in the general two-Higgs-doublet model, Phys. Rev. D **64**, 014014 (2001).

[2] B. H. Behrens *et al.* (CLEO Collaboration), Two-Body B Meson Decays to η and η': Observation of $B \rightarrow \eta' K$, Phys. Rev. Lett. **80**, 3710 (1998).

[3] K. A. Olive *et al.* (Particle Data Group), Review of particle physics, Chin. Phys. C **38**, 090001 (2014).

[4] B. Aubert *et al.* (*BABAR* Collaboration), B meson decays to charmless meson pairs containing η or η' mesons, Phys. Rev. D **80**, 112002 (2009).

[5] J. Schumann *et al.* (Belle Collaboration), Evidence for $B \rightarrow \eta' \pi$ and Improved Measurements for $B \rightarrow \eta' K$, Phys. Rev. Lett. **97**, 061802 (2006).

[6] B. Aubert *et al.* (*BABAR* Collaboration), Measurement of time dependent *CP* asymmetry parameters in B^0 meson decays to ωK_S^0, $\eta' K^0$, and $\pi^0 K_{(S)}^0$, Phys. Rev. D **79**, 052003 (2009).

[7] K.-F. Chen *et al.* (Belle Collaboration), Observation of Time-Dependent *CP* Violation in $B^0 \rightarrow \eta' K^0$ Decays and Improved Measurements of *CP* Asymmetries in $B^0 \rightarrow \phi K^0$, $K_S^0 K_S^0 K_S^0$ and $B^0 \rightarrow J/\psi K^0$, Phys. Rev. Lett. **98**, 031802 (2007).

[8] M. Acciarri *et al.* (L3 Collaboration), Search for neutral charmless B decays at LEP, Phys. Lett. B **363**, 127 (1995).

[9] K. Abe *et al.* (SLD Collaboration), Search for charmless hadronic decays of B mesons with the SLD detector, Phys. Rev. D **62**, 071101 (2000).

[10] H.-Y. Cheng and C.-K. Chua, QCD factorization for charmless hadronic B_s^0 decays revisited, Phys. Rev. D **80**, 114026 (2009).

[11] J. Sun, G. Zhu, and D. Du, Phenomenological analysis of charmless decays $B_{(s)} \rightarrow PP$, PV, with QCD factorization, Phys. Rev. D **68**, 054003 (2003).

[12] M. Beneke and M. Neubert, QCD factorization for $B \rightarrow PP$ and $B \rightarrow PV$ decays, Nucl. Phys. **B675**, 333 (2003).

[13] A. Ali, G. Kramer, Y. Li, C.-D. Lü, Y.-L. Shen, W. Wang, and Y.-M. Wang, Charmless non-leptonic B_s^0 decays to PP, PV and VV final states in the perturbative QCD approach, Phys. Rev. D **76**, 074018 (2007).

[14] A. R. Williamson and J. Zupan, Two body B decays with isosinglet final states in SCET, Phys. Rev. D **74**, 014003 (2006).

[15] H.-Y. Cheng, C.-W. Chiang, and A.-L. Kuo, Updating $B \rightarrow PP$, VP decays in the framework of flavor symmetry, Phys. Rev. D **91**, 014011 (2015).

[16] R. Aaij *et al.* (LHCb Collaboration), Measurement of *CP* violation in $B_s^0 \rightarrow \phi\phi$ decays, Phys. Rev. D **90**, 052011 (2014).

[17] A. A. Alves, Jr. *et al.*, The LHCb detector at the LHC, JINST **3**, S08005 (2008).

[18] R. Aaij *et al.* (LHCb Collaboration), The LHCb trigger and its performance in 2011, JINST **8**, P04022 (2013).

[19] G. Punzi, Sensitivity of searches for new signals and its optimization, *Proceedings of the "PHYSTAT2003," SLAC, Stanford, California, 2003*, edited by L. Lyons, R. Mount, and R. Reitmeyer, eConf C030908, 79 (2003).

[20] R. Aaij *et al.* (LHCb Collaboration), LHCb detector performance, Int. J. Mod. Phys. A **30**, 1530022 (2015).

[21] T. Skwarnicki, Ph.D. thesis, Institute of Nuclear Physics, Krakow, 1986 [Report No. DESY-F31-86-02].

[22] H. Albrecht *et al.* (ARGUS Collaboration), Search for $b \rightarrow s\gamma$ in exclusive decays of B mesons, Phys. Lett. B **229**, 304 (1989).

[23] S. S. Wilks, The large-sample distribution of the likelihood ratio for testing composite hypotheses, Ann. Math. Stat. **9**, 60 (1938).

[24] R. Aaij *et al.* (LHCb Collaboration), Measurement of the fragmentation fraction ratio f_s/f_d and its dependence on B meson kinematics, J. High Energy Phys. 04 (2013) 001; LHCb Collaboration, Average f_s/f_d b-Hadron Production Fraction Ratio for 7 TeV pp Collisions, Report No. LHCb-CONF-2013-011.

[25] R. Aaij *et al.* (LHCb Collaboration), Evidence for the decay $B^0 \rightarrow J/\psi\omega$ and measurement of the relative branching fractions of B_s^0 meson decays to $J/\psi\eta$ and $J/\psi\eta'$, Nucl. Phys. **B867**, 547 (2013).

[26] R. Aaij *et al.* (LHCb Collaboration), Measurement of the charge asymmetry in $B^\pm \rightarrow \phi K^\pm$ and search for $B^\pm \rightarrow \phi\pi^\pm$ decays, Phys. Lett. B **728**, 85 (2014).

[27] H.-n. Li and S. Mishima, Penguin-dominated $B \rightarrow PV$ decays in NLO perturbative QCD, Phys. Rev. D **74**, 094020 (2006).

R. Aaij,[41] B. Adeva,[37] M. Adinolfi,[46] A. Affolder,[52] Z. Ajaltouni,[5] S. Akar,[6] J. Albrecht,[9] F. Alessio,[38] M. Alexander,[51] S. Ali,[41] G. Alkhazov,[30] P. Alvarez Cartelle,[37] A. A. Alves Jr.,[25,38] S. Amato,[2] S. Amerio,[22] Y. Amhis,[7] L. An,[3] L. Anderlini,[17,a] J. Anderson,[40] R. Andreassen,[57] M. Andreotti,[16,b] J. E. Andrews,[58] R. B. Appleby,[54] O. Aquines Gutierrez,[10] F. Archilli,[38] A. Artamonov,[35] M. Artuso,[59] E. Aslanides,[6] G. Auriemma,[25,c] M. Baalouch,[5] S. Bachmann,[11] J. J. Back,[48] A. Badalov,[36] C. Baesso,[60] W. Baldini,[16] R. J. Barlow,[54] C. Barschel,[38] S. Barsuk,[7] W. Barter,[38] V. Batozskaya,[28] V. Battista,[39] A. Bay,[39] L. Beaucourt,[4] J. Beddow,[51] F. Bedeschi,[23] I. Bediaga,[1] L. J. Bel,[41] S. Belogurov,[31] K. Belous,[35] I. Belyaev,[31] E. Ben-Haim,[8] G. Bencivenni,[18] S. Benson,[38] J. Benton,[46] A. Berezhnoy,[32] R. Bernet,[40] A. Bertolin,[22] M.-O. Bettler,[47] M. van Beuzekom,[41] A. Bien,[11] S. Bifani,[45] T. Bird,[54] A. Bizzeti,[17,d] T. Blake,[48] F. Blanc,[39] J. Blouw,[10] S. Blusk,[59] V. Bocci,[25] A. Bondar,[34] N. Bondar,[30,38] W. Bonivento,[15] S. Borghi,[54] A. Borgia,[59] M. Borsato,[7] T. J. V. Bowcock,[52] E. Bowen,[40] C. Bozzi,[16] D. Brett,[54] M. Britsch,[10] T. Britton,[59] J. Brodzicka,[54] N. H. Brook,[46] A. Bursche,[40] J. Buytaert,[38] S. Cadeddu,[15] R. Calabrese,[16,b] M. Calvi,[20,e] M. Calvo Gomez,[36,f] P. Campana,[18] D. Campora Perez,[38] L. Capriotti,[54] A. Carbone,[14,g] G. Carboni,[24,h] R. Cardinale,[19,38,i] A. Cardini,[15] L. Carson,[50] K. Carvalho Akiba,[2,38] R. Casanova Mohr,[36] G. Casse,[52] L. Cassina,[20,e] L. Castillo Garcia,[38] M. Cattaneo,[38] Ch. Cauet,[9] G. Cavallero,[19] R. Cenci,[23,j] M. Charles,[8] Ph. Charpentier,[38] M. Chefdeville,[4] S. Chen,[54] S.-F. Cheung,[55] N. Chiapolini,[40] M. Chrzaszcz,[40,26] X. Cid Vidal,[38] G. Ciezarek,[41] P. E. L. Clarke,[50] M. Clemencic,[38] H. V. Cliff,[47] J. Closier,[38] V. Coco,[38] J. Cogan,[6] E. Cogneras,[5] V. Cogoni,[15,k] L. Cojocariu,[29] G. Collazuol,[22] P. Collins,[38] A. Comerma-Montells,[11] A. Contu,[15,38] A. Cook,[46] M. Coombes,[46] S. Coquereau,[8] G. Corti,[38] M. Corvo,[16,b] I. Counts,[56] B. Couturier,[38] G. A. Cowan,[50] D. C. Craik,[48] A. C. Crocombe,[48] M. Cruz Torres,[60] S. Cunliffe,[53] R. Currie,[53] C. D'Ambrosio,[38] J. Dalseno,[46] P. David,[8] P. N. Y. David,[41] A. Davis,[57] K. De Bruyn,[41] S. De Capua,[54] M. De Cian,[11] J. M. De Miranda,[1] L. De Paula,[2] W. De Silva,[57] P. De Simone,[18] C.-T. Dean,[51] D. Decamp,[4] M. Deckenhoff,[9] L. Del Buono,[8] N. Déléage,[4] D. Derkach,[55] O. Deschamps,[5] F. Dettori,[38] B. Dey,[40] A. Di Canto,[38] H. Dijkstra,[38] S. Donleavy,[52] F. Dordei,[11] M. Dorigo,[39] A. Dosil Suárez,[37] D. Dossett,[48] A. Dovbnya,[43] K. Dreimanis,[52] G. Dujany,[54] F. Dupertuis,[39] P. Durante,[6] R. Dzhelyadin,[35] A. Dziurda,[26] A. Dzyuba,[30] S. Easo,[49,38] U. Egede,[53] V. Egorychev,[31] S. Eidelman,[34] S. Eisenhardt,[50] U. Eitschberger,[9] R. Ekelhof,[9] L. Eklund,[51] I. El Rifai,[5] Ch. Elsasser,[40] S. Ely,[59] S. Esen,[11] H. M. Evans,[47] T. Evans,[55] A. Falabella,[14] C. Färber,[11] C. Farinelli,[41] N. Farley,[45] S. Farry,[52] R. Fay,[52] D. Ferguson,[50] V. Fernandez Albor,[37] F. Ferrari,[14] F. Ferreira Rodrigues,[1] M. Ferro-Luzzi,[38] S. Filippov,[33] M. Fiore,[16,b] M. Fiorini,[16,b] M. Firlej,[27] C. Fitzpatrick,[39] T. Fiutowski,[27] P. Fol,[53] M. Fontana,[10] F. Fontanelli,[19,i] R. Forty,[38] O. Francisco,[2] M. Frank,[38] C. Frei,[38] M. Frosini,[17] J. Fu,[21,38] E. Furfaro,[24,h] A. Gallas Torreira,[37] D. Galli,[14,g] S. Gallorini,[22,38] S. Gambetta,[19,i] M. Gandelman,[2] P. Gandini,[59] Y. Gao,[3] J. García Pardiñas,[37] J. Garofoli,[59] J. Garra Tico,[47] L. Garrido,[36] D. Gascon,[36] C. Gaspar,[38] U. Gastaldi,[16] R. Gauld,[55] L. Gavardi,[9] G. Gazzoni,[5] A. Geraci,[21,l] D. Gerick,[11] E. Gersabeck,[11] M. Gersabeck,[54] T. Gershon,[48] Ph. Ghez,[4] A. Gianelle,[22] S. Gianì,[39] V. Gibson,[47] L. Giubega,[29] V. V. Gligorov,[38] C. Göbel,[60] D. Golubkov,[31] A. Golutvin,[53,31,38] A. Gomes,[1,m] C. Gotti,[20,e] M. Grabalosa Gándara,[5] R. Graciani Diaz,[36] L. A. Granado Cardoso,[38] E. Graugés,[36] E. Graverini,[40] G. Graziani,[17] A. Grecu,[29] E. Greening,[55] S. Gregson,[47] P. Griffith,[45] L. Grillo,[11] O. Grünberg,[63] B. Gui,[59] E. Gushchin,[33] Yu. Guz,[35,38] T. Gys,[38] C. Hadjivasiliou,[59] G. Haefeli,[39] C. Haen,[38] S. C. Haines,[47] S. Hall,[53] B. Hamilton,[58] T. Hampson,[46] X. Han,[11] S. Hansmann-Menzemer,[11] N. Harnew,[55] S. T. Harnew,[46] J. Harrison,[54] J. He,[38] T. Head,[39] V. Heijne,[41] K. Hennessy,[52] P. Henrard,[5] L. Henry,[8] J. A. Hernando Morata,[37] E. van Herwijnen,[38] M. Heß,[63] A. Hicheur,[2] D. Hill,[55] M. Hoballah,[5] C. Hombach,[54] W. Hulsbergen,[41] N. Hussain,[55] D. Hutchcroft,[52] D. Hynds,[51] M. Idzik,[27] P. Ilten,[56] R. Jacobsson,[38] A. Jaeger,[11] J. Jalocha,[55] E. Jans,[41] A. Jawahery,[58] F. Jing,[3] M. John,[55] D. Johnson,[38] C. R. Jones,[47] C. Joram,[38] B. Jost,[38] N. Jurik,[59] S. Kandybei,[43] W. Kanso,[6] M. Karacson,[38] T. M. Karbach,[38] S. Karodia,[51] M. Kelsey,[59] I. R. Kenyon,[45] M. Kenzie,[38] T. Ketel,[42] B. Khanji,[20,38,e] C. Khurewathanakul,[39] S. Klaver,[54] K. Klimaszewski,[28] O. Kochebina,[7] M. Kolpin,[11] I. Komarov,[39] R. F. Koopman,[42] P. Koppenburg,[41,38] M. Korolev,[32] L. Kravchuk,[33] K. Kreplin,[11] M. Kreps,[48] G. Krocker,[11] P. Krokovny,[34] F. Kruse,[9] W. Kucewicz,[26,n] M. Kucharczyk,[20,e] V. Kudryavtsev,[34] K. Kurek,[28] T. Kvaratskheliya,[31] V. N. La Thi,[39] D. Lacarrere,[38] G. Lafferty,[54] A. Lai,[15] D. Lambert,[50] R. W. Lambert,[42] G. Lanfranchi,[18] C. Langenbruch,[48] B. Langhans,[38] T. Latham,[48] C. Lazzeroni,[45] R. Le Gac,[6] J. van Leerdam,[41] J.-P. Lees,[4] R. Lefèvre,[5] A. Leflat,[32] J. Lefrançois,[7] O. Leroy,[6] T. Lesiak,[26] B. Leverington,[11] Y. Li,[7] T. Likhomanenko,[64] M. Liles,[52] R. Lindner,[38] C. Linn,[38] F. Lionetto,[40] B. Liu,[15] S. Lohn,[38] I. Longstaff,[51] J. H. Lopes,[2] P. Lowdon,[40] D. Lucchesi,[22,o] H. Luo,[50] A. Lupato,[22] E. Luppi,[16,b] O. Lupton,[55] F. Machefert,[7] I. V. Machikhiliyan,[31] F. Maciuc,[29] O. Maev,[30] S. Malde,[55] A. Malinin,[64] G. Manca,[15,k] G. Mancinelli,[6] P. Manning,[59] A. Mapelli,[38] J. Maratas,[5] J. F. Marchand,[4] U. Marconi,[14] C. Marin Benito,[36] P. Marino,[23,j] R. Märki,[39] J. Marks,[11] G. Martellotti,[25] M. Martinelli,[39] D. Martinez Santos,[42] F. Martinez Vidal,[65] D. Martins Tostes,[2] A. Massafferri,[1]

R. Matev,[38] Z. Mathe,[38] C. Matteuzzi,[20] B. Maurin,[39] A. Mazurov,[45] M. McCann,[53] J. McCarthy,[45] A. McNab,[54] R. McNulty,[12] B. McSkelly,[52] B. Meadows,[57] F. Meier,[9] M. Meissner,[11] M. Merk,[41] D. A. Milanes,[62] M.-N. Minard,[4] D. S. Mitzel,[11] J. Molina Rodriguez,[60] S. Monteil,[5] M. Morandin,[22] P. Morawski,[27] A. Mordà,[6] M. J. Morello,[23,j] J. Moron,[27] A.-B. Morris,[50] R. Mountain,[59] F. Muheim,[50] K. Müller,[40] M. Mussini,[14] B. Muster,[39] P. Naik,[46] T. Nakada,[39] R. Nandakumar,[49] I. Nasteva,[2] M. Needham,[50] N. Neri,[21] S. Neubert,[38] N. Neufeld,[38] M. Neuner,[11] A. D. Nguyen,[39] T. D. Nguyen,[39] C. Nguyen-Mau,[39,p] M. Nicol,[7] V. Niess,[5] R. Niet,[9] N. Nikitin,[32] T. Nikodem,[11] A. Novoselov,[35] D. P. O'Hanlon,[48] A. Oblakowska-Mucha,[27] V. Obraztsov,[35] S. Ogilvy,[51] O. Okhrimenko,[44] R. Oldeman,[15,k] C. J. G. Onderwater,[66] B. Osorio Rodrigues,[1] J. M. Otalora Goicochea,[2] A. Otto,[38] P. Owen,[53] A. Oyanguren,[65] B. K. Pal,[59] A. Palano,[13,q] F. Palombo,[21,r] M. Palutan,[18] J. Panman,[38] A. Papanestis,[49,38] M. Pappagallo,[51] L. L. Pappalardo,[16,b] C. Parkes,[54] C. J. Parkinson,[9,45] G. Passaleva,[17] G. D. Patel,[52] M. Patel,[53] C. Patrignani,[19,i] A. Pearce,[54,49] A. Pellegrino,[41] G. Penso,[25,s] M. Pepe Altarelli,[38] S. Perazzini,[14,g] P. Perret,[5] L. Pescatore,[45] K. Petridis,[53] A. Petrolini,[19,i] E. Picatoste Olloqui,[36] B. Pietrzyk,[4] T. Pilař,[48] D. Pinci,[25] A. Pistone,[19] S. Playfer,[50] M. Plo Casasus,[37] F. Polci,[8] A. Poluektov,[48,34] I. Polyakov,[31] E. Polycarpo,[2] A. Popov,[35] D. Popov,[10] B. Popovici,[29] C. Potterat,[2] E. Price,[46] J. D. Price,[52] J. Prisciandaro,[39] A. Pritchard,[52] C. Prouve,[46] V. Pugatch,[44] A. Puig Navarro,[39] G. Punzi,[23,t] W. Qian,[4] R. Quagliani,[7,46] B. Rachwal,[26] J. H. Rademacker,[46] B. Rakotomiaramanana,[39] M. Rama,[23] M. S. Rangel,[2] I. Raniuk,[43] N. Rauschmayr,[38] G. Raven,[42] F. Redi,[53] S. Reichert,[54] M. M. Reid,[48] A. C. dos Reis,[1] S. Ricciardi,[49] S. Richards,[46] M. Rihl,[38] K. Rinnert,[52] V. Rives Molina,[36] P. Robbe,[7] A. B. Rodrigues,[1] E. Rodrigues,[54] P. Rodriguez Perez,[54] S. Roiser,[38] V. Romanovsky,[35] A. Romero Vidal,[37] M. Rotondo,[22] J. Rouvinet,[39] T. Ruf,[38] H. Ruiz,[36] P. Ruiz Valls,[65] J. J. Saborido Silva,[37] N. Sagidova,[30] P. Sail,[51] B. Saitta,[15,k] V. Salustino Guimaraes,[2] C. Sanchez Mayordomo,[65] B. Sanmartin Sedes,[37] R. Santacesaria,[25] C. Santamarina Rios,[37] E. Santovetti,[24,h] A. Sarti,[18,s] C. Satriano,[25,c] A. Satta,[24] D. M. Saunders,[46] D. Savrina,[31,32] M. Schiller,[38] H. Schindler,[38] M. Schlupp,[9] M. Schmelling,[10] B. Schmidt,[38] O. Schneider,[39] A. Schopper,[38] M.-H. Schune,[7] R. Schwemmer,[38] B. Sciascia,[18] A. Sciubba,[25,s] A. Semennikov,[31] I. Sepp,[53] N. Serra,[40] J. Serrano,[6] L. Sestini,[22] P. Seyfert,[11] M. Shapkin,[35] I. Shapoval,[16,43,b] Y. Shcheglov,[30] T. Shears,[52] L. Shekhtman,[34] V. Shevchenko,[64] A. Shires,[9] R. Silva Coutinho,[48] G. Simi,[22] M. Sirendi,[47] N. Skidmore,[46] I. Skillicorn,[51] T. Skwarnicki,[59] N. A. Smith,[52] E. Smith,[55,49] E. Smith,[53] J. Smith,[47] M. Smith,[54] H. Snoek,[41] M. D. Sokoloff,[57] F. J. P. Soler,[51] F. Soomro,[39] D. Souza,[46] B. Souza De Paula,[2] B. Spaan,[9] P. Spradlin,[51] S. Sridharan,[38] F. Stagni,[38] M. Stahl,[11] S. Stahl,[38] O. Steinkamp,[40] O. Stenyakin,[35] F. Sterpka,[59] S. Stevenson,[55] S. Stoica,[29] S. Stone,[59] B. Storaci,[40] S. Stracka,[23,j] M. Straticiuc,[29] U. Straumann,[40] R. Stroili,[22] L. Sun,[57] W. Sutcliffe,[53] K. Swientek,[27] S. Swientek,[9] V. Syropoulos,[42] M. Szczekowski,[28] P. Szczypka,[39,38] T. Szumlak,[27] S. T'Jampens,[4] M. Teklishyn,[7] G. Tellarini,[16,b] F. Teubert,[38] C. Thomas,[55] E. Thomas,[38] J. van Tilburg,[41] V. Tisserand,[4] M. Tobin,[39] J. Todd,[57] S. Tolk,[42] L. Tomassetti,[16,b] D. Tonelli,[38] S. Topp-Joergensen,[55] N. Torr,[55] E. Tournefier,[4] S. Tourneur,[39] K. Trabelsi,[39] M. T. Tran,[39] M. Tresch,[40] A. Trisovic,[38] A. Tsaregorodtsev,[6] P. Tsopelas,[41] N. Tuning,[41] M. Ubeda Garcia,[38] A. Ukleja,[28] A. Ustyuzhanin,[64] U. Uwer,[11] C. Vacca,[15,k] V. Vagnoni,[14] G. Valenti,[14] A. Vallier,[7] R. Vazquez Gomez,[18] P. Vazquez Regueiro,[37] C. Vázquez Sierra,[37] S. Vecchi,[16] J. J. Velthuis,[46] M. Veltri,[17,u] G. Veneziano,[39] M. Vesterinen,[11] J. V. Viana Barbosa,[38] B. Viaud,[7] D. Vieira,[2] M. Vieites Diaz,[37] X. Vilasis-Cardona,[36,f] A. Vollhardt,[40] D. Volyanskyy,[10] D. Voong,[46] A. Vorobyev,[30] V. Vorobyev,[34] C. Voß,[63] J. A. de Vries,[41] R. Waldi,[63] C. Wallace,[48] R. Wallace,[12] J. Walsh,[23] S. Wandernoth,[11] J. Wang,[59] D. R. Ward,[47] N. K. Watson,[45] D. Websdale,[53] M. Whitehead,[48] D. Wiedner,[11] G. Wilkinson,[55,38] M. Wilkinson,[59] M. P. Williams,[45] M. Williams,[56] F. F. Wilson,[49] J. Wimberley,[58] J. Wishahi,[9] W. Wislicki,[28] M. Witek,[26] G. Wormser,[7] S. A. Wotton,[47] S. Wright,[47] K. Wyllie,[38] Y. Xie,[61] Z. Xing,[59] Z. Xu,[39] Z. Yang,[3] X. Yuan,[34] O. Yushchenko,[35] M. Zangoli,[14] M. Zavertyaev,[10,v] L. Zhang,[3] W. C. Zhang,[12] Y. Zhang,[3] A. Zhelezov,[11] A. Zhokhov,[31] and L. Zhong[3]

(LHCb Collaboration)

[1]Centro Brasileiro de Pesquisas Físicas (CBPF), Rio de Janeiro, Brazil
[2]Universidade Federal do Rio de Janeiro (UFRJ), Rio de Janeiro, Brazil
[3]Center for High Energy Physics, Tsinghua University, Beijing, China
[4]LAPP, Université Savoie Mont-Blanc, CNRS/IN2P3, Annecy-Le-Vieux, France
[5]Clermont Université, Université Blaise Pascal, CNRS/IN2P3, LPC, Clermont-Ferrand, France
[6]CPPM, Aix-Marseille Université, CNRS/IN2P3, Marseille, France
[7]LAL, Université Paris-Sud, CNRS/IN2P3, Orsay, France
[8]LPNHE, Université Pierre et Marie Curie, Université Paris Diderot, CNRS/IN2P3, Paris, France

[9]*Fakultät Physik, Technische Universität Dortmund, Dortmund, Germany*
[10]*Max-Planck-Institut für Kernphysik (MPIK), Heidelberg, Germany*
[11]*Physikalisches Institut, Ruprecht-Karls-Universität Heidelberg, Heidelberg, Germany*
[12]*School of Physics, University College Dublin, Dublin, Ireland*
[13]*Sezione INFN di Bari, Bari, Italy*
[14]*Sezione INFN di Bologna, Bologna, Italy*
[15]*Sezione INFN di Cagliari, Cagliari, Italy*
[16]*Sezione INFN di Ferrara, Ferrara, Italy*
[17]*Sezione INFN di Firenze, Firenze, Italy*
[18]*Laboratori Nazionali dell'INFN di Frascati, Frascati, Italy*
[19]*Sezione INFN di Genova, Genova, Italy*
[20]*Sezione INFN di Milano Bicocca, Milano, Italy*
[21]*Sezione INFN di Milano, Milano, Italy*
[22]*Sezione INFN di Padova, Padova, Italy*
[23]*Sezione INFN di Pisa, Pisa, Italy*
[24]*Sezione INFN di Roma Tor Vergata, Roma, Italy*
[25]*Sezione INFN di Roma La Sapienza, Roma, Italy*
[26]*Henryk Niewodniczanski Institute of Nuclear Physics Polish Academy of Sciences, Kraków, Poland*
[27]*AGH - University of Science and Technology, Faculty of Physics and Applied Computer Science, Kraków, Poland*
[28]*National Center for Nuclear Research (NCBJ), Warsaw, Poland*
[29]*Horia Hulubei National Institute of Physics and Nuclear Engineering, Bucharest-Magurele, Romania*
[30]*Petersburg Nuclear Physics Institute (PNPI), Gatchina, Russia*
[31]*Institute of Theoretical and Experimental Physics (ITEP), Moscow, Russia*
[32]*Institute of Nuclear Physics, Moscow State University (SINP MSU), Moscow, Russia*
[33]*Institute for Nuclear Research of the Russian Academy of Sciences (INR RAN), Moscow, Russia*
[34]*Budker Institute of Nuclear Physics (SB RAS) and Novosibirsk State University, Novosibirsk, Russia*
[35]*Institute for High Energy Physics (IHEP), Protvino, Russia*
[36]*Universitat de Barcelona, Barcelona, Spain*
[37]*Universidad de Santiago de Compostela, Santiago de Compostela, Spain*
[38]*European Organization for Nuclear Research (CERN), Geneva, Switzerland*
[39]*Ecole Polytechnique Fédérale de Lausanne (EPFL), Lausanne, Switzerland*
[40]*Physik-Institut, Universität Zürich, Zürich, Switzerland*
[41]*Nikhef National Institute for Subatomic Physics, Amsterdam, The Netherlands*
[42]*Nikhef National Institute for Subatomic Physics and VU University Amsterdam, Amsterdam, The Netherlands*
[43]*NSC Kharkiv Institute of Physics and Technology (NSC KIPT), Kharkiv, Ukraine*
[44]*Institute for Nuclear Research of the National Academy of Sciences (KINR), Kyiv, Ukraine*
[45]*University of Birmingham, Birmingham, United Kingdom*
[46]*H.H. Wills Physics Laboratory, University of Bristol, Bristol, United Kingdom*
[47]*Cavendish Laboratory, University of Cambridge, Cambridge, United Kingdom*
[48]*Department of Physics, University of Warwick, Coventry, United Kingdom*
[49]*STFC Rutherford Appleton Laboratory, Didcot, United Kingdom*
[50]*School of Physics and Astronomy, University of Edinburgh, Edinburgh, United Kingdom*
[51]*School of Physics and Astronomy, University of Glasgow, Glasgow, United Kingdom*
[52]*Oliver Lodge Laboratory, University of Liverpool, Liverpool, United Kingdom*
[53]*Imperial College London, London, United Kingdom*
[54]*School of Physics and Astronomy, University of Manchester, Manchester, United Kingdom*
[55]*Department of Physics, University of Oxford, Oxford, United Kingdom*
[56]*Massachusetts Institute of Technology, Cambridge, Massachusetts 02139, USA*
[57]*University of Cincinnati, Cincinnati, Ohio 45221, USA*
[58]*University of Maryland, College Park, Maryland 20742, USA*
[59]*Syracuse University, Syracuse, New York 13224, USA*
[60]*Pontifícia Universidade Católica do Rio de Janeiro (PUC-Rio), Rio de Janeiro, Brazil (associated with Universidade Federal do Rio de Janeiro (UFRJ), Rio de Janeiro, Brazil)*
[61]*Institute of Particle Physics, Central China Normal University, Wuhan, Hubei, China (associated with Center for High Energy Physics, Tsinghua University, Beijing, China)*
[62]*Departamento de Fisica, Universidad Nacional de Colombia, Bogota, Colombia (associated with LPNHE, Université Pierre et Marie Curie, Université Paris Diderot, CNRS/IN2P3, Paris, France)*
[63]*Institut für Physik, Universität Rostock, Rostock, Germany (associated with Physikalisches Institut, Ruprecht-Karls-Universität Heidelberg, Heidelberg, Germany)*

[64]National Research Centre Kurchatov Institute, Moscow, Russia (associated with
Institute of Theoretical and Experimental Physics (ITEP), Moscow, Russia)
[65]Instituto de Fisica Corpuscular (IFIC), Universitat de Valencia-CSIC, Valencia,
Spain (associated with Universitat de Barcelona, Barcelona, Spain)
[66]Van Swinderen Institute, University of Groningen, Groningen, The Netherlands (associated with
Nikhef National Institute for Subatomic Physics, Amsterdam, The Netherlands)

[a]Also at Università di Firenze, Firenze, Italy.
[b]Also at Università di Ferrara, Ferrara, Italy.
[c]Also at Università della Basilicata, Potenza, Italy.
[d]Also at Università di Modena e Reggio Emilia, Modena, Italy.
[e]Also at Università di Milano Bicocca, Milano, Italy.
[f]Also at LIFAELS, La Salle, Universitat Ramon Llull, Barcelona, Spain.
[g]Also at Università di Bologna, Bologna, Italy.
[h]Also at Università di Roma Tor Vergata, Roma, Italy.
[i]Also at Università di Genova, Genova, Italy.
[j]Also at Scuola Normale Superiore, Pisa, Italy.
[k]Also at Università di Cagliari, Cagliari, Italy.
[l]Also at Politecnico di Milano, Milano, Italy.
[m]Also at Universidade Federal do Triângulo Mineiro (UFTM), Uberaba-MG, Brazil.
[n]Also at AGH - University of Science and Technology, Faculty of Computer Science, Electronics and Telecommunications, Kraków,
Poland.
[o]Also at Università di Padova, Padova, Italy.
[p]Also at Hanoi University of Science, Hanoi, Viet Nam.
[q]Also at Università di Bari, Bari, Italy.
[r]Also at Università degli Studi di Milano, Milano, Italy.
[s]Also at Università di Roma La Sapienza, Roma, Italy.
[t]Also at Università di Pisa, Pisa, Italy.
[u]Also at Università di Urbino, Urbino, Italy.
[v]Also at P.N. Lebedev Physical Institute, Russian Academy of Science (LPI RAS), Moscow, Russia.